Dusan Nesic*, Tomislav Milosevic and Branko Kolundzija

Ultra wideband bandpass filters with specified relative bandwidth

https://doi.org/10.1515/freq-2021-0034
Received February 3, 2021; accepted October 8, 2021;
published online October 25, 2021

Abstract: Algorithm for the realization of the broad range of values of wide relative bandwidth (*RBW*) bandpass filter is introduced. Algorithm is based on periodic ideal cells each with short-ended stub. Theory is developed for a symmetrical cell with proportional transmission lines, nonuniform or uniform, in term of characteristic impedance. The theory is applied for the uniform transmission lines. Simple equation of the ratio between characteristic impendence of the short-ended stub and the characteristic impendences of the main lines is given for the broad range of *RBW*. Realizable filters are for the very wide *RBW* up to over 1.5 (150%). Technology is chosen in microstrip with vias for the short ends. It is without coupling, without defected ground structure (DGS) and only with a single layer. The procedure is tested on the fabricated filters for very wide *RBW* of 1.5 (150%). Agreement between measurements and simulations is excellent.

Keywords: filter design; microstrip; microwave; periodic structure; ultra wideband bandpass filter.

1 Introduction

Wide bandpass filters are important part of microwave systems [1–4]. Many of them are for ultra wideband communications spectrum from 3.1 to 10.6 GHz with relative bandwidth (*RBW*) around 1.1 [1, 4]. All of them are assumed to suppress DC and lower frequencies. It can be done using coupling and short-ended stubs [1–4] or only short-ended stubs [5–9]. Majority of them are done in microstrip technology, the most use planar technology in microwave systems. Some of them are also using defected ground structure (DGS), coupling or multilayers [1, 4]. General problem is that there is no specific realizable algorithm procedure for the very wide *RBW*. The table in [10, Table 6.1] gives, for example for 4 cells, characteristic impedance of short-ended stub over 150 Ω for *RBW* = 1.33 and even over 200 Ω for *RBW* = 1.44. Value of 150 Ω as the characteristic impedance of stubs can be realizable for the common teflon substrates (i.e. d = 0.508 mm, ε_r = 2.1) but very hard for thinner substrates or higher ε_r.

This paper introduces a realizable algorithm for the range of values of *RBW* up to over 1.50 using only short-ended stubs. The algorithm is based on the periodical array of cells. Theory is developed for a symmetrical cell, nonuniform or uniform, with proportional transmission lines in term of characteristic impedance. The theory is applied for the uniform transmission lines. For the filter of *RBW* = 1.50 the optimized stub impedance is of the realizable 123.4 Ω. Even all stub impedances for *RBW* = 1.50 are managed to be the same in contrast to the various values in [10]. Fabrication technology is the single layer microstrip. The structure is without coupling and without defected ground structure (DGS). The procedure is tested on the fabricated filter for *RBW* = 1.5.

2 Theory

Considered general structure of the ideal lossless unit cell is shown in Figure 1. It is something similar to the cell for low-pass filter with open-ended shunt network in [11]. The shunt network in this paper is short-ended. All cell networks are described, as in [11], in the form of ABCD matrix. The cell consists of three networks: two networks (N1 and N2) are cascaded and one network is shunted and short-ended (N3). Network N2 is the same as N1 except that the roles of its ports are reversed, so that $A_t = D$, $B_t = B$, $C_t = C$, and $D_t = A$. Effectively, two identical networks of ABCD-parameters (A, B, C and D) are cascaded back to back at port ⑤ with the shunt network of ABCD-parameters A_s, B_s, C_s, and D_s, whose other port ⑥ is short-ended. In fact it is one T-junction. The cell is symmetrical but networks can be nonuniform or uniform transmission lines.

***Corresponding author: Dusan Nesic**, Centre of Microelectronic Technologies, Institute of Chemistry, Technology and Metallurgy, University of Belgrade, Njegoseva 12, Belgrade, Serbia, E-mail: nesicad@nanosys.ihtm.bg.ac.rs
Tomislav Milosevic, WIPL-D d.o.o., Gandijeva 7, 11073 Belgrade, Serbia, E-mail: tomislav.milosevic@wipl-d.com
Branko Kolundzija, School of Electrical Engineering, University of Belgrade, 73 Bulevar kralja Aleksandra, 11020 Belgrade, Serbia, E-mail: kol@etf.rs

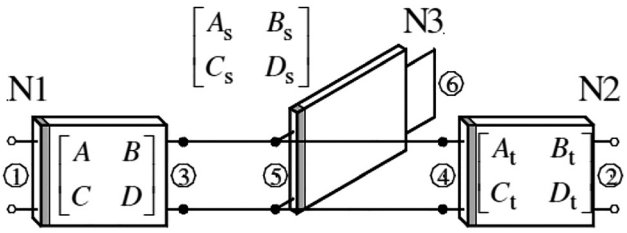

Figure 1: Scheme of a filter cell with ABCD matrix.

The shunt short-ended network N3 acts as a shunt admittance $Y_s = D_s/B_s$ at port ⑤, so it can be replaced by a two-port network of ABCD-parameters 1, 0, Y_s and 1 between ports ③ and ④ in Figure 2. Matrix with Y_s is developed in (1).

$$\begin{bmatrix} 1 & 0 \\ Y_s & 1 \end{bmatrix} = \begin{bmatrix} 1 & 0 \\ \frac{D_s}{B_s} & 1 \end{bmatrix} \tag{1}$$

Developed matrix of the completed cell ($A_cB_cC_cD_c$) is presented in (2)

$$\begin{bmatrix} A_c & B_c \\ C_c & D_c \end{bmatrix} = \begin{bmatrix} A & B \\ C & D \end{bmatrix} \cdot \begin{bmatrix} 1 & 0 \\ \frac{D_s}{B_s} & 1 \end{bmatrix} \cdot \begin{bmatrix} D & B \\ C & A \end{bmatrix}$$
$$= \begin{bmatrix} AD + BC + \frac{D_s}{B_s}BD & 2AB + \frac{D_s}{B_s}B^2 \\ 2CD + \frac{D_s}{B_s}D^2 & AD + BC + \frac{D_s}{B_s}BD \end{bmatrix} \tag{2}$$

In an infinite cascade of the identical unit cells the wave propagates along the structure only if $|(A_c + D_c)/2| \le 1$ [12], which implies existence of passbands of the structure. Symmetrical cell, $A_c = D_c$, simply implies $|A_c| \le 1$. After arranging matrix the final condition for the passband is in (3)

$$-1 \le AD + BC + \frac{D_sBD}{B_s} \le 1 \tag{3}$$

Incorporating reciprocity $AD - BC = 1$ then (3) becomes (4)

$$0 \le 2AD + \frac{D_sBD}{B_s} \le 2 \tag{4}$$

Take attention on D_sBD/B_s. In the center of the stopband B_s is changing the sign through value of 0 and the admittance, $Y_s = D_s/B_s$, is in infinity. In the center of the pass band is $Y_s = 0$ for $D_s = 0$.

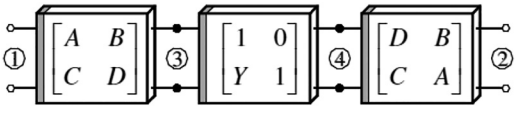

Figure 2: Developed scheme of a filter cell with ABCD matrix.

If product D_sBD does not have 0 in the same frequency as B_s the whole expression is changing between minus infinity and plus infinity. It produces fast changing of passbands and stopbands. One way to prevent that is solution with equal electrical lengths for all networks N1, N3 and N2 in Figure 1. In the same time, the solution need proportional characteristics impedances Z on network N1 and Z_s on short-ended network N3 on distance θ from the beginning of each network as in (5)

$$\frac{Z(\theta)}{Z_s(\theta)} = k \tag{5}$$

Applying proportion (5) mathematical induction can proves relation between parameters of the networks

$$A_s = A \quad D_s = D \quad B_s = B/k \quad C_s = kC \tag{6}$$

Now all is in the form of ABCD paramaters of the N1 network. Then relation (4) can be written as

$$0 \le (2A + kD)D \le 2 \tag{7}$$

If network N1 is considered symmetrical, $A = D$, (7) becomes (8) and depends only on A^2 and k

$$0 \le 2A^2 + kA^2 \le 2 \tag{8}$$

Relation (8) is always positive. For $\theta = 0$ and lower θ it is a stopband. $2A^2 + kA^2 = 2$ corresponds to the beginning $A(\theta_{c1})$ and the end $A(\theta_{c2})$ of the passband. θ_{c1} and θ_{c2} is the first pair of θ which satisfy the equation. Periodicity is π. The proportion (5) of the characteristic impedances k depends on θ_{c1} and θ_{c2} through A^2.

$$\frac{Z(\theta)}{Z_s(\theta)} = k = 2\left(\frac{1}{A(\theta_{c1})^2} - 1\right) \tag{9}$$

In fact, if the beginning of the passband θ_{c1} is known it determines the proportion $k = Z(\theta)/Z_s(\theta)$. Equalizing (8) with 0 determines $A = 0$ for the middle of the bandpass. It is also valid, according to (6) and symmetry of N1, for the short-ended network N3, $A = D = A_s = D_s = 0$.

For the filter formed by cascade of identical unit cells it is important to match nominal impendence of ports (commonly $Z_0 = 50\ \Omega$) as much as possible. It was done by matching Bloch impendence to the nominal impendence Z_0. Bloch impenance Z_B is calculated as

$$Z_B = \sqrt{\frac{B_c}{C_c}} = \sqrt{\frac{(2+k)B^2}{(2+k)A^2 - 2}} \tag{10}$$

In final, the cell in Figure 1 in an infinite cascade of identical unit cells is a symmetrical cell. The whole cell is determinated over ABCD parameters of the network N1. The network N2 is symmetrical to the N1 and the short-ended

network N3 is equal electrical length and proportional to N1 in term of the characteristic impedance. The network N1 is symmetrical but can be a nonuniform or a uniform transmission line.

3 Algorithm for the uniform transmission lines

The shape of the cell with $\theta_s = \theta$ and the uniform transmission lines is presented in Figure 3.

In the case of the networks as uniform transmission lines ABCD parameters of the N1 network become

$$\begin{bmatrix} A & B \\ C & D \end{bmatrix} = \begin{bmatrix} \cos\theta & jZ\sin\theta \\ \frac{j}{Z}\sin\theta & \cos\theta \end{bmatrix} \tag{11}$$

For the N3 network are

$$\begin{bmatrix} A_s & B_s \\ C_s & D_s \end{bmatrix} = \begin{bmatrix} \cos\theta_s & jZ_s\sin\theta_s \\ \frac{j}{Z_s}\sin\theta_s & \cos\theta_s \end{bmatrix} \tag{12}$$

Condition for the passband (8) becomes

$$-1 \le -1 + 2\cos(\theta)^2 + \cos(\theta)^2\frac{Z}{Z_s} \le 1 \tag{13}$$

Diagram of (13) in Figure 4 is done for an arbitrary ratio Z/Z_s. Relation (7) has a period π and is presented in the phase range from 0 to π. The result of the relation (13) is in the range between –1 and +1 and corresponds to the bandpass region.

As can be seen in Figure 4, center of the bandpass region logically corresponds to $\theta_s = \pi/2$. Boundaries of the bandpass are signed with θ_{c1} for the lower frequency and θ_{c2} for the higher frequency. According to the mentioned one can calculate useful bandpass filter characteristics. Relation between boundaries is $\theta_{c2} = \pi - \theta_{c1}$ and θ_{c1} will be

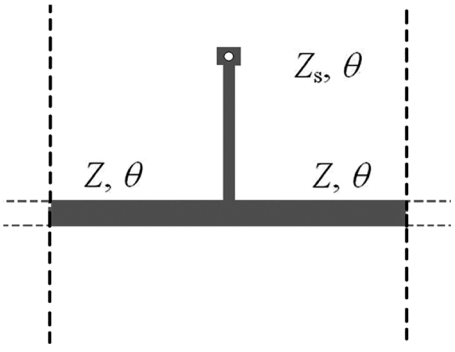

Figure 3: A unit cell made of uniform transmission lines of equal lengths, $\theta_s = \theta$.

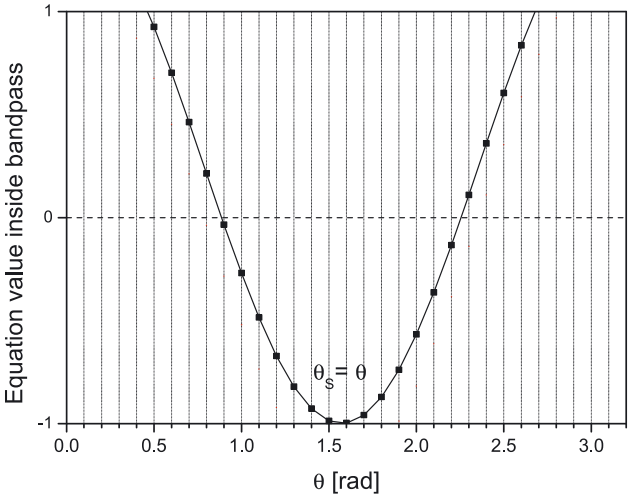

Figure 4: Value of (13) inside bandpass region versus θ for an arbitrary ratio Z/Z_s.

replace in equations simply with θ_c. Relative bandwidth (*RBW*) of the bandpass is

$$RBW = \frac{\theta_{c2} - \theta_{c1}}{\frac{1}{2}(\theta_{c1} + \theta_{c2})} = 2 - \frac{4}{\pi}\theta_{c1} = 2 - \frac{4}{\pi}\theta_c \tag{14}$$

$$\theta_c = \frac{2 - RBW}{4}\pi \tag{15}$$

For $RWB = 2$ value of θ_c becomes 0 and $Z/Z_s = k = 0$ (Z_s approaches infinity). The proportion k in (9) for the characteristic impedances for the lower *RWB* becomes

$$k = \frac{Z}{Z_s} = 2\,tg^2(\theta_c) \tag{16}$$

For the given *RBW* one can calculate boundary θ_c from (15) and next calculate Z/Z_s from (16). Dependence of (Z/Z_s) versus *RBW* is presented in Figure 5 in a calibration curve. For better view presentation is for $Z/Z_s > 1$ or $Z_s/Z > 1$.

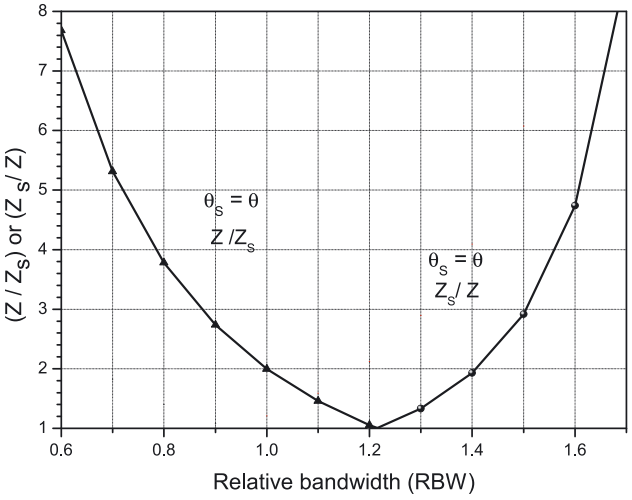

Figure 5: Calibration curve: dependence of Z/Z_s or Z_s/Z versus *RBW*.

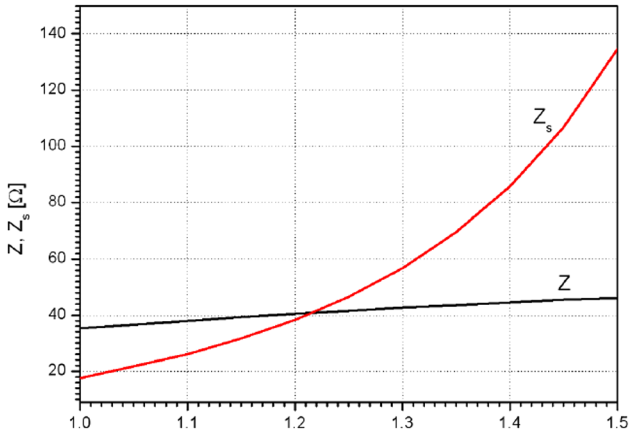

Figure 6: Dependence of Z and Z_s versus *RBW* for Bloch impendence of 50 Ω.

According to Figure 5 very high *RBW* needs huge ratio between Z_s and Z and it is not realizable. The same is valid for the narrow *RBW*. Realizable *RBW* in microstrip technology is good for a wideband bandpass filter below *RBW* = 1.6. Ratio $Z_s/Z > 1$ corresponds to relatively narrow stub microstrip line and is easier for realization of T-junction close to ideal. The Bloch impedance in (10) gives

$$Z_B = \frac{Z}{\cos\theta_c \sqrt{1 - \left(\frac{\cot\theta}{\cot\theta_c}\right)^2}} \tag{17}$$

As can be seen Bloch impendence is equal to $Z/\cos(\theta_c)$ for the center of the band-pass filter $\theta = \pi/2$, $\cot(\pi/2) = 0$. It means that Z in the simulation process has the start value of $Z = Z_0\cos(\theta_c)$ and need to be optimized for the whole band-pass. Dependence of Z and Z_s versus *RBW* for the Bloch impendence is presented in Figure 6. The procedure from the given *RBW*, to the value of Z according to the Bloch impedance (Z_0 = 50 Ω) and the value of Z_s, is presented as an algorithm in (18)

$$\theta_c = \frac{2 - RBW}{4}\pi \quad Z = Z_0\cos(\theta_c) \quad \frac{Z}{Z_s} = 2tg^2(\theta_c) \quad \text{(18a, b, c)}$$

The high characteristic impedances Z_s for the very wide *RBW* are much smaller and realizable in comparation to the same *RBW* from [10]: Z_s = 65 Ω versus over 150 Ω for *RBW* = 1.33 and Z_s = 134.6 Ω versus over 250 Ω for *RBW* = 1.50 (Over 250 Ω is by interpolation from the element values presented in the table in [10]).

4 Application to filter

Using previously developed equations ideal 4-cells filters are simulated for *RBW* = 1.5 (150%), 1.33 (133%) and 1.0 (100%) around central frequency of 3 GHz. Ideal model is presented in Figure 7 for four identical cells with correspondence between $\pi/2$ and $\lambda/4$ (L/λ = 0.250 in Figure 7). Simulation is done in program package WIPL-D [13]. The Bloch calculations for the nominal 50 Ω give: for *RBW* = 1.5 are Z = 46.2 Ω and Z_s = 134.6 Ω, for *RBW* = 1.33 are Z = 43.3 Ω and Z_s = 65 Ω and for *RBW* = 1.00 are Z = 35.4 Ω and Z_s = 17.7 Ω. Wider RWB gives easy realizable characteristic impedances in contrast to very low impedance Z_s = 17.7 Ω for *RBW* = 1.00.

Simulated results for four identical cells are presented in Figure 8a and b. As can be seen, S_{11} parameters are better for the wider band-stop-filters. Logically, using Bloch calculation (18), S_{11} parameters are totally matched only for the central frequency (3 GHz in Figure 8a) and much higher on the boundaries. Optimization is in direction of equalizing maximums of the S_{11} parameters in the whole band-pass region. In order to do that impendence Z calculated in (18) need to be something lower. New optimized results are presented in Figure 9a and b. Optimized results are for the case with equal values of S_{11} for the first, sixth, third and fourth maximums in the bandpass, Figure 9a. Optimized values for *RBW* = 1.5 are Z = 42.4 Ω and Z_s = 123.4 Ω and for *RBW* = 1.00 are Z = 28.5 Ω and Z_s = 14.25 Ω. Optimizations were done manually.

Steepness of the filter is better for more cells but more cells induce a longer structure. One cell longitudinal dimension is $\lambda/2$. 4-cells filter is chosen as optimal and for −3 dB criteria *RBW* is shifted only 3%. The wider filters have also the better S_{11} parameters. Even all stubs for the specified *RBW* are managed to be of the same value of the characteristic impedance which is easier for the fabrication.

5 Validation

Validation for $\theta_s = \theta$ is realized in microstrip technique on substrate FR-4, thickness d = 1.5 mm, relative dielectric constant ε_r = 4.6 (obtained from the company that fabricated the structure) and $tg\ \delta$ = 0.02. It is a 4-cells filter with *RBW* = 1.5 around central frequency of 3 GHz (from 0.75 to 5.25 GHz). Microstrip electromagnetic (EM) model is presented in Figure 10 in program package WIPL-D [13]. The short-ended stubs correspond to a quarter of the guided wavelength ($\lambda_g/4$) are realized using metallized vias. Its comparison with the ideal model is presented in Figure 11. Electromagnetic model has inserted losses, S_{21}, induced by dielectric losses of $tg\ \delta$ = 0.02. It induces relative non-agreement in higher frequency edge of the filter. Agreement

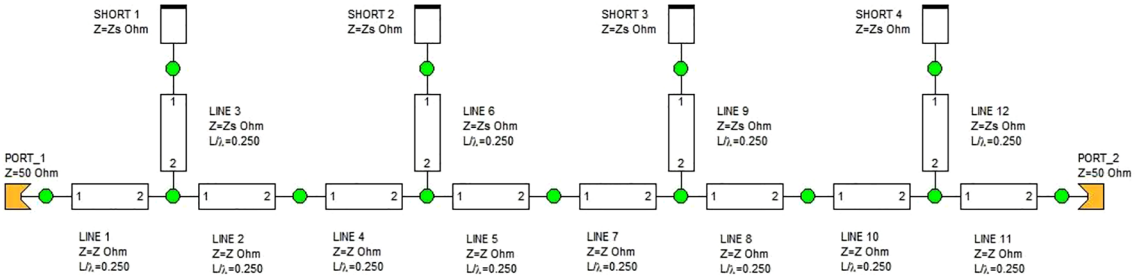

Figure 7: Ideal model of a 4-cells filter with identical cells.

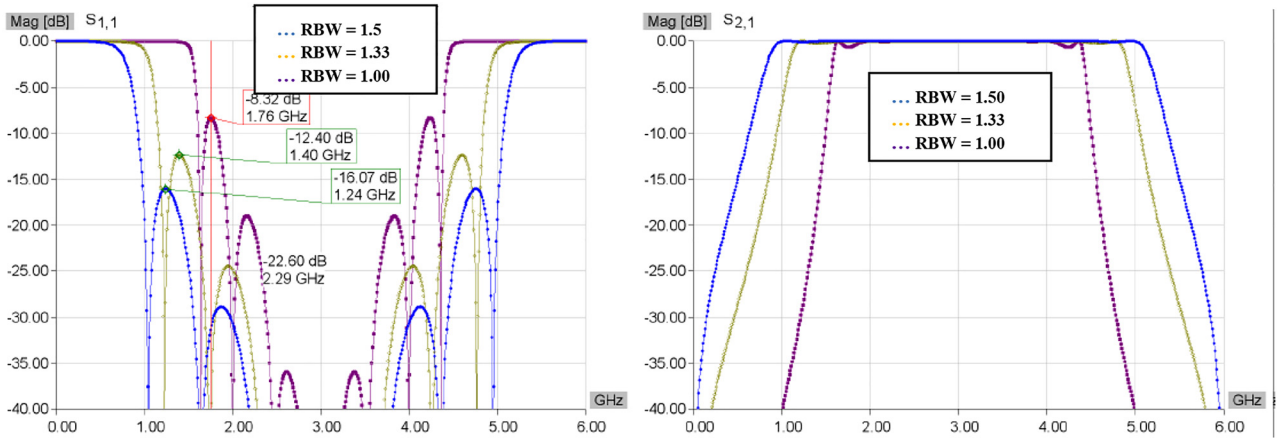

Figure 8: a, b: Three wideband filters in the ideal model of 4 cells according to Bloch impedance (15).

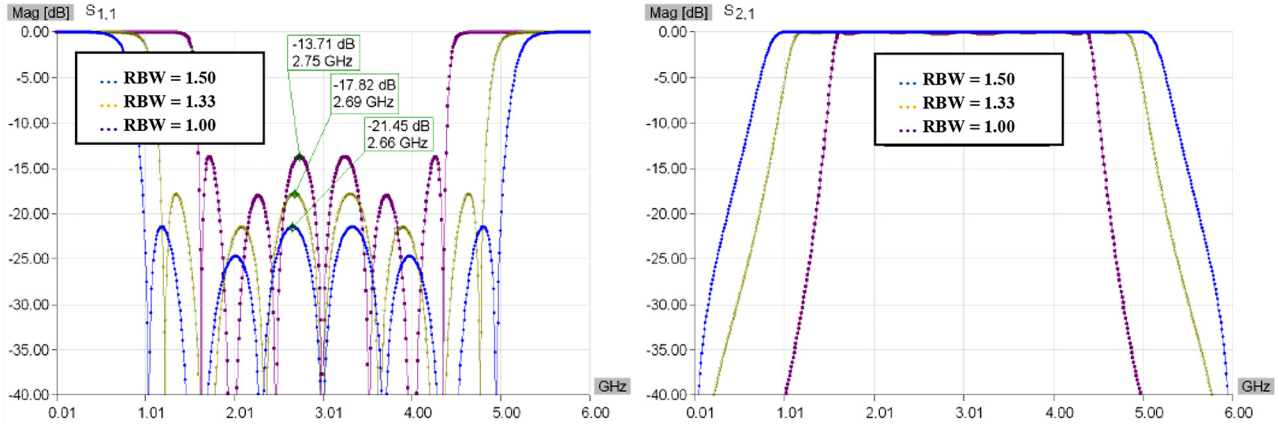

Figure 9: a, b: Three wideband filters in the ideal model of 4 cells with something lower *Z*.

is very good in the low frequency edge. S_{11} is in a relative agreement.

Fabricated model of the filter is presented in Figure 12. Measured results in comparison with EM model are presented in Figure 13. After the measurement, we determined that it is correct to put $\varepsilon_r = 4.3$ instead of initially obtained $\varepsilon_r = 4.6$. Because of this, the EM simulation in Figure 13 is slightly shifted towards higher frequencies. There is a very good agreement in S_{21} parameters between measured results and EM model even at higher frequencies. It is a very good agreement with modeling of losses. There are some small ripples above 4 GHz in S_{21} measurement. S_{11} parameters are

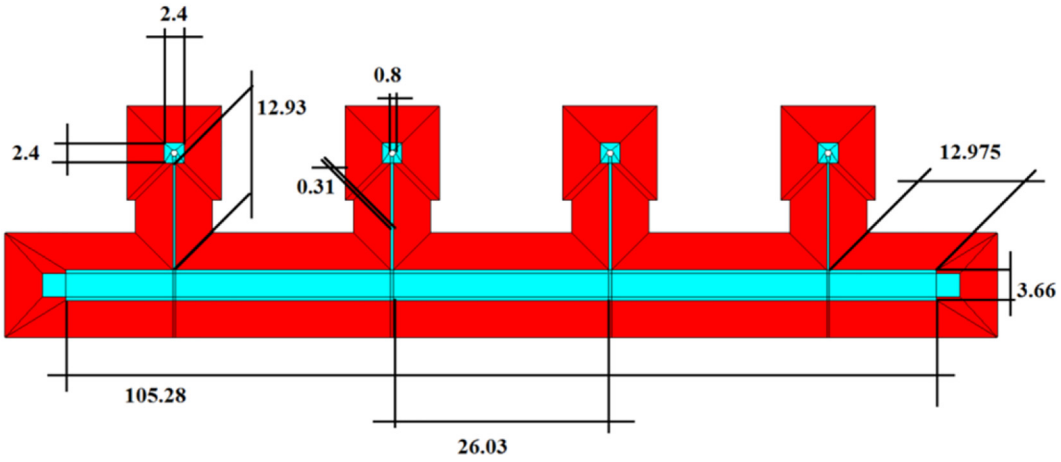

Figure 10: Electromagnetic model in WIPL-D. Dimensions are in mm. The ports are on 50 Ω short narrower lines (narrower than 42.4 Ω) at the both ends.

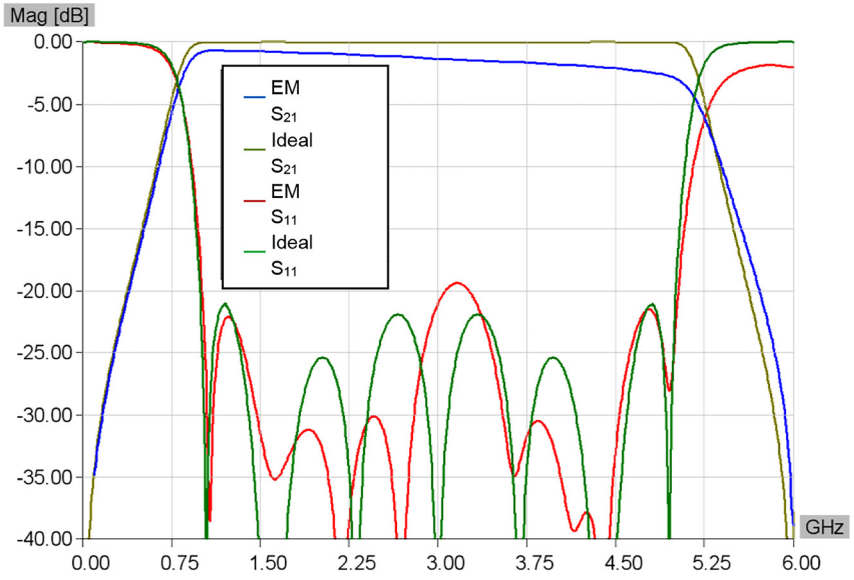

Figure 11: Characteristics of the filter in ideal and electromagnetic model.

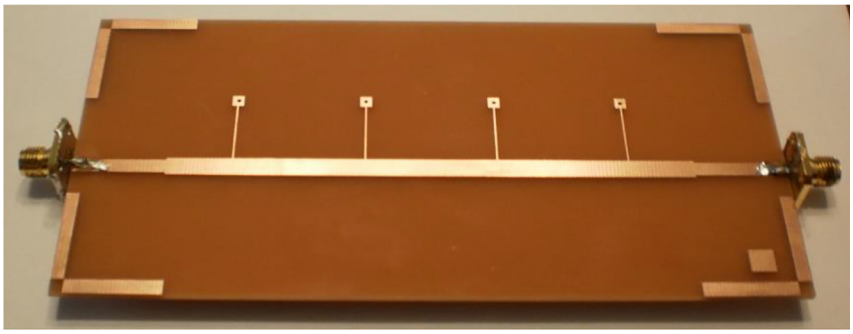

Figure 12: Fabricated prototype of the filter.

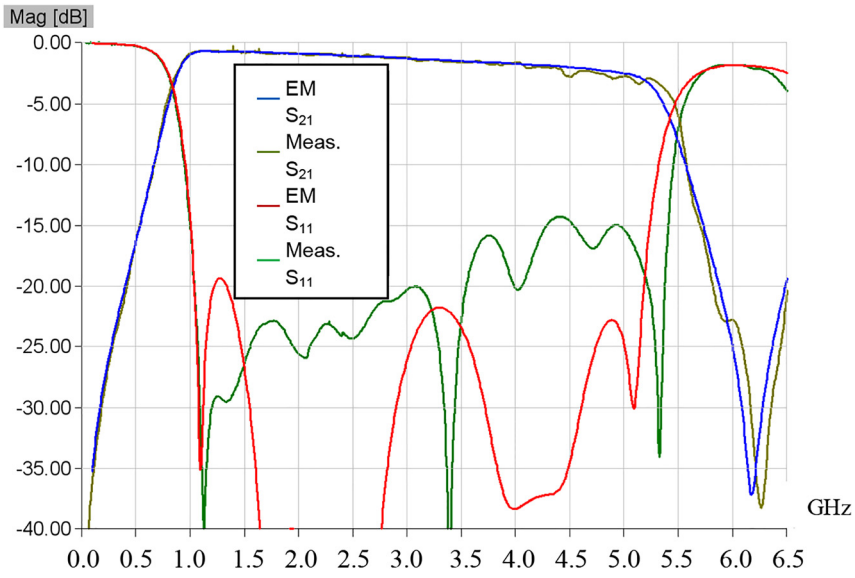

Figure 13: Characteristics of the measured filter and electromagnetic model.

in disagreement especially in high at higher frequencies but have accepted values, significantly lower than –10 dB.

6 Conclusions

This paper first presents algorithm for the broad range of values of bandpass filters with ultra wide relative bandwidth (*RBW*) up to over 1.50 (150%). The algorithm is based on periodic ideal identical cells each with a short-ended stub. First, it was explained for the case of a symmetrical cell with proportional transmission lines in term of characteristic impedance. In general case transmission lines are symmetrical and nonuniform. The theory is applied to the uniform transmission lines.

The procedure from the given *RBW* to the value of Z according to the Bloch impedance ($Z_0 = 50\ \Omega$) and finally the value of Z_s, is presented through simple equations. Characteristic impendences are at first calculated according to the Bloch impedance and then slightly optimized for the optimal S_{11} parameters in the whole bandpass region of the filter. Tables are not needed. Design curve of the ratio between characteristic impendences of the short-ended stub and characteristic impendences of the main lines is also given for the broad range of values of *RBW*. The advantages are realizable (fabricable) characteristic impedances of the short-ended stubs for very wide bandpass filters, wider than around 1.30 (130%). The high characteristic impedances Z_s for the very wide *RBW* are much smaller and realizable in comparation to the same *RBW* from the literature. Dimension of one cell equals $\lambda/2 \times \lambda/4$, where λ is the wavelength of the central frequency of the first bandpass.

Technology is chosen in microstrip with vias for the short ends. The structure is without coupling and without defected ground structure (DGS). The procedure is tested on the fabricated filters for very wide bandpass *RBW* = 1.50 (150%). Agreement between measured filter and electromagnetic model for S_{21} is excellent. Measured S_{11} have accepted values, significantly lower than –10 dB. Even all stubs are managed to be of the same value of the characteristic impedance which is good for fabrication.

Along with microstrip the algorithm can be also applied to stripline and coplanar waveguide (CPW).

Author contributions: All the authors have accepted responsibility for the entire content of this submitted manuscript and approved submission.
Research funding: This work was financially supported by Ministry of Education, Science and Technological Development of the Republic of Serbia (Grant No. 451-03-68/2020-14/200026).
Conflict of interest statement: The authors declare no conflicts of interest regarding this article.

References

[1] Z.-C. Hao and J.-S. Hong, "Ultrawideband filter technologies," *IEEE Microw. Mag.*, vol. 11, no. 4, pp. 56–68, 2010.
[2] R. Zhang and D. Peroulis, "Planar multifrequency wideband bandpass filters with constant and frequency mappings," *IEEE Trans. Microw. Theor. Tech.*, vol. 66, no. 2, pp. 935–942, 2018.
[3] R. Zhang, S. Luo, and L. Zhu, "A new synthesis and design method for wideband bandpass filters with generalized unit

elements," *IEEE Trans. Microw. Theor. Tech.*, vol. 65, no. 3, pp. 815–823, 2017.
[4] L.-T. Wang, Y. Xiong, and M. He, *Review on UWB Bandpass Filters, UWB Technology – Circuits and Systems*, London, Mohamed Kheir, IntechOpen, 2019. Available at: https://www.intechopen.com/books/uwb-technology-circuits-and-systems/review-on-uwb-bandpass-filters.
[5] M. S. Razalli, A. Ismail, M. A. Mahd, and M. N. Hamidon, "Compact configuration ultra-wideband microwave filter using quarter-wave length short-circuited stub," in *Proceedings of Asia-Pacific Microwave Conference 2007*, Bangkok, Thailand, 2007.
[6] J.-S. Hong and H. Shaman, "An optimum ultra-wideband microstrip filter," *Microw. Opt. Technol. Lett.*, vol. 47, no. 3, pp. 230–233, 2005.
[7] W.-T. Wong, Y.-S. Lin, C.-H. Wang, and C. H. Chen, "Highly selective microstrip bandpass filters for ultra-wideband (UWB) applications," in *Proceedings of Asia-Pacific Microwave Conference 2005*, Suzhou, China, 2005.
[8] M. S. Razalli, A. Ismail, M. A. Mahdi, and M. N. Hamidon, "Ultra-wide band microwave filter utilizing quarter-wavelength short-circuited stubs," *Microw. Opt. Technol. Lett.*, vol. 50, no. 11, pp. 2981–2983, 2008.
[9] M. S. Razalli, A. Ismail, M. A. Mahdi, and M. N. Hamidon, "Compact ultra-wide band microwave filter utilizing quarter-wave length short circuited stubs with reduced number of vias," *Microw. Opt. Technol. Lett.*, vol. 51, no. 9, pp. 2116–2119, 2009.
[10] J.-S. Hong, *Microstrip Filters for RF/Microwave Applications*, Hoboken, New Jersey, John Wiley and Sons, 2011.
[11] D. A. Nesic, B. M. Kolundzija, D. V. Tosic, and D. S. Jeremic, "Low-pass filter with deep and wide stop band and controllable rejection bandwidth," *Int. J. Microw Wirel. Technol.*, vol. 7, no. 2, pp. 141–149, 2015.
[12] D. M. Pozar, *Microwave Engineering*, New York, John Wiley and Sons, 1998.
[13] *Program Package WIPL-D Pro v15*, Belgrade, WIPL-D d.o.o., 2019. Available at: www.wipl-d.com.